

Non-LTE dust nucleation in sub-saturated vapors

Davide Lazzati

JILA, University of Colorado, 440 UCB, Boulder, CO 80309-0440, USA

25 October 2018

ABSTRACT

We use the kinetic theory of nucleation to explore the properties of dust nucleation in sub-saturated vapors. Due to radiation losses, the sub-critical clusters have a smaller temperature compared to their vapor. This alters the dynamical balance between attachment and detachment of monomers, allowing for stable nucleation of grains in vapors that are sub-saturated for their temperature. We find this effect particularly important at low densities and in the absence of a strong background radiation field. We find new conditions for stable nucleation in the n – T phase diagram. The nucleation in the non-LTE regions is likely to be at much slower rate than in the super-saturated vapors. We evaluate the nucleation rate, warning the reader that it does depend on poorly substantiated properties of the macro-molecules assumed in the computation. On the other hand, the conditions for nucleation depend only on the properties of the large stable grains and are more robust. We finally point out that this mechanism may be relevant in the early universe as an initial dust pollution mechanism, since once the interstellar medium is polluted with dust, mantle growth is likely to be dominant over non-LTE nucleation in the diffuse medium.

Key words: dust, extinction

1 INTRODUCTION

Dust particles are one of the fundamental components of the interstellar medium (ISM) and an ever-present worry for observers due to their opacity at optical and UV wavelengths (Cardelli, Clayton & Mathis 1989). The ISM of the Milky Way is polluted by a mixture of grains made of a variety of materials, likely dominated by carbonaceous grains, silicates, and small PAHs particles (Mathis, Rumpl & Nordsieck 1977; Weingartner & Draine 2001). The dust properties are supposed to be the result of dust formation in the outflows of evolved stars (e.g. Salpeter 1977; Stein & Soifer 1983; Mathis 1990; Whittet 1992; Draine 2003, and references therein) and subsequent evolution, and eventual dissolution, in the ISM, mainly as the effect of shock waves that destroy the grains through sputtering (Draine 1989; McKee 1989; Edmunds 2001). Alternative dust production sites are supernova explosions (Kozasa, Hasegawa & Nomoto 1989, 1991; Todini & Ferrara 2001; Nozawa et al. 2003; Schneider, Ferrara & Salvaterra 2004; Bianchi & Schneider 2007) and quasar outflows (Elvis, Marengo & Karovska, 2002).

The theory of dust nucleation in astrophysics is heavily influenced by the theory of the nucleation of phase transitions in super-saturated vapors (Becker & Doring 1935; Feder et al. 1966; Abraham 1974). The theory had mild success in reproducing nucleation rates, but is still controversial in many aspects, especially because it extrapolates the properties of macroscopic bodies to clusters of few molecules and

because it extends the thermodynamic approach to systems with a handful of particles. To add to these problems, astrophysical dust nucleation requires chemical reactions, since grains of materials that do not have a vapor state do nucleate (think, for example, to the nucleation of olivines from silicon oxides and metals; Draine 1979; Gail & Sedlmayr 1986). An alternative approach is the so-called kinetic theory, which describes nucleation as the result of attachment and detachment of monomers from a seed cluster of n particles (atoms, molecules or radicals; Nowakowski & Ruckenstein 1991ab).

Both the thermodynamic and the kinetic nucleation theory have been developed in conditions of *true equilibrium*, i.e., when the two phases have the same temperature. In the astrophysical scenario, however, the temperature of the dust grains can be sensibly lower than the temperature of the gas in which they are embedded due to efficient radiation cooling (e.g., Draine 1981). This would seem to be irrelevant to nucleation theory, since a vapor needs to be already nucleated in order to have grains that can be colder than the gas phase. Even a sub-saturated vapor, however, has a large number of unstable clusters that form by random association of monomers (and rapidly evaporate). In this paper we study the effect of cooling of these proto-clusters in a sub-saturated vapor, and the effect this has on the balance between attachment and detachment of monomers. Using the kinetic theory of nucleation, we find that even largely sub-saturated vapors can nucleate, provided they are not immersed in a strong radiation field. We compute, albeit

under some controversial assumptions, the non-LTE nucleation rate. We show that, even though it is not as large as in super-saturated vapors, it can produce dust grains at a rate that can reproduce the average dust grain density in the Milky Way over a timescale of several million years. In addition we show that non-LTE effects can increase the nucleation rate in super-saturated vapors. Non-LTE nucleation could therefore provide a slow channel for dust formation, in which dust is built over a relative long time in a slowly evolving region. Such an example could be the outflow from AGN nuclei (Elvis et al. 2002). Such evolution is different from the one envisaged in the classical dust factories – AGB star atmospheres and supernovæ – where dust nucleation is rapid but short lived since the favorable conditions are rapidly lost.

This paper is organized as follows: in § 2 we briefly review the classical kinetic theory of nucleation; in § 3 we compute the dust grain temperature and in § 4 we compute the new conditions for nucleation. In § 5 we consider the nucleation rate and discuss our results in § 6.

2 CLASSICAL NUCLEATION

In this section we review some basic concepts of the theory of nucleation at densities and temperatures typical of laboratory experiments (in conditions of “true equilibrium”). Let us first consider a flat surface separating the vapor phase of a certain material with its condensed phase (either liquid or solid). The equilibrium condition between the two phases can be described in either thermodynamic or kinetic terms.

In thermodynamic terms, equilibrium implies that the temperature of the two phases are equal and that the chemical potential of the molecules in the two phases are equal (e.g., Vehkamäki 2006). In this paper we adopt the kinetic approach, since we will investigate nucleation out of thermal equilibrium. In the kinetic representation the equilibrium is dynamical and is obtained by equating the rate of vapor phase molecules that become attached to the condensed phase to the rate of molecules that return from the condensed phase to the vapor. The first rate is relatively easy to quantify, as long as it can be assumed that the vapor molecule velocity distribution is Maxwellian¹:

$$\frac{dn_{\text{in}}}{dt dA} = k_s n_X \sqrt{\frac{kT}{2\pi m_X}} \quad (1)$$

where n_X is the density of the molecules (or atoms) of the compound of interest in the vapor phase, k is the Boltzmann constant, T is the temperature and m_X the molecular mass. The parameter $k_s \leq 1$ is the sticking coefficient and represents the probability that the incoming monomer remains attached to the condensed phase rather than bounce and return to the vapor. There is no reason for k_s to be constant and it does indeed depend on the temperature (see, e.g., Batista et al. 2005). For the sake of simplicity, we will consider here k_s to be a constant.

The rate of detachment of monomers from the condensed phase is much harder - if at all possible - to compute

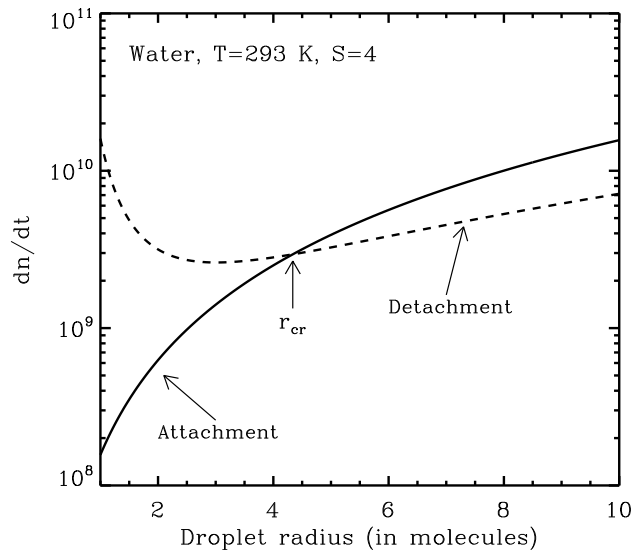


Figure 1. The attachment and detachment of monomers from a water droplet at $T = 293$ K and saturation $S = 4$. The solid curve shows the attachment rate, while the dashed curve shows the detachment rate as a function of the droplet radius. At small radii, the detachment dominates and the droplet tends to evaporate. At large radii, the attachment dominates and the drop tends to grow in size. There exist a radius where the rates are equal and the droplet is stable. This is called the critical radius r_{cr} , and the droplet, called critical cluster, contains a critical number of monomers.

a-priori. It can be obtained by comparing the experimentally determined saturation density $n_{X,\text{eq}}(T)$ with the theoretical attachment rate from Eq. 1 (see, e.g., Kashchiev 2000, hereinafter K00, and references therein):

$$\frac{dn_{\text{out}}}{dt dA} = k_s n_{X,\text{eq}}(T) \sqrt{\frac{kT}{2\pi m_X}} \quad (2)$$

Equation 2, which is formally identical to Eq. 1, becomes interesting if we assume that the detachment rate from the condensed phase does not depend on the properties of the vapor phase (pressure, temperature, saturation). This seems to be a good assumption, since the properties and dynamics of a condensed material should be rather independent from the low-density gas surrounding it. However, the detachment rate may depend slightly on the vapor conditions (pressure, temperature, density) through their effect on the properties of the condensed material (density, conductivity, surface tension). We neglect here these dependencies since there is no established theory to model them. With this assumption, Eq. 2 give us the detachment rate as a function of the properties of the condensed phase only, as long as the saturation density as a function of temperature is known either theoretically or experimentally.

So far we discussed the equilibrium between a flat surface and a vapor. Phase transitions cannot take place in a single bulk event, but must be realized through microscopical nucleation of the new phase, due to energetic constraints (K00). Equation 2 is modified if the surface that separate the vapor from the condensed phase is not flat. Let us consider a spherical droplet of radius r . Both thermodynamic (Vehkamäki 2006) and kinetic consideration (K00)

¹ We concentrate here on homogeneous nucleation in vapors with only inert species and the compound of interest.

show that the saturation density for a droplet is larger than for a flat surface. In the thermodynamic case, this is due to the surface energy component, while in the kinetic approach, the effect can be explained through the fact that the binding energy of a surface monomer is smaller than for a bulk one, and so it is easier to eject a monomer for a small droplet than for a flat surface (at the same temperature). As long as the number of molecules in the droplet is large enough to allow for the definition of a surface, it can be shown that (K00):

$$n_{X,\text{eq}}(r, T) = n_{X,\text{eq}}(T) e^{\frac{2\sigma v_0}{rkT}} \quad (3)$$

where σ is the surface tension of the condensed phase and v_0 the volume occupied by one molecule in the condensed phase. Since the rate of impacts of vapor molecules on the surface does not depend on the curvature, and assuming that the sticking coefficient does not either, we can easily find the detachment rate as a function of temperature as:

$$\frac{dn_{\text{out}}(r)}{dt dA} = k_s n_{X,\text{eq}}(T) \sqrt{\frac{kT}{2\pi m_X}} e^{\frac{2\sigma v_0}{rkT}} \quad (4)$$

where we used the so-called capillary approximation, i.e., we assume that σ does not depend on r . Even though not explicit, the ejection rate of Eq. 4 depends strongly on the grain temperature through the equilibrium density $n_{X,\text{eq}}(T)$. The equilibrium density depends exponentially on the temperature, roughly as $n_{X,\text{eq}}(T) \propto e^{-A/kT}$, where A is a positive, material dependent, constant.

Figure 1 compares the attachment and detachment rates of monomers for water droplets at a temperature $T = 293 \text{ K}$ and at saturation $S = n_X/n_{X,\text{eq}} = 4$. We adopted $\sigma = 78 \text{ dyne/cm}$, $v_0 = m_{\text{H}_2\text{O}}/\rho = 3 \times 10^{-23} \text{ cm}^3$, $k_s = 1$, and we obtained the equilibrium pressure from the ChERIC (Chemical Engineering Research Information Center) web site². At small radii, the detachment rate is larger than the attachment rate and the droplet will tend to evaporate, while at large radii the droplet tends to grow. At the critical radius r_{cr} the two rates are equal and the droplet is in equilibrium. The droplet with this radius is also called *critical cluster*. It is easy to see that the problem of nucleation reduces to the difficulty of creating droplets big enough to be super-critical, since once the critical radius is passed, the droplet will grow into the condensed phase.

The fact that a droplet (or nucleus) smaller than r_{cr} tends to evaporate does not mean that it is impossible to nucleate in the absence of pre-existing super-critical droplets. It exists, in fact, the possibility that by statistical fluctuations a nucleus grows big enough to reach the critical radius and subsequently evolve in a stable droplet. For a super-saturated vapor, it can be shown that the stationary distribution of nuclei is given by (K00 and references therein):

$$\frac{dN}{dn} = n_X \frac{\prod_{i=1}^{n-1} f_i}{\prod_{i=2}^n g_i} \left[1 + \sum_{i=2}^{\infty} \left(\prod_{j=2}^i \frac{g_j}{f_j} \right) \right]^{-1} \sum_{i=n}^{\infty} \left(\prod_{j=2}^i \frac{g_j}{f_j} \right) \quad (5)$$

where n is the number of molecules in the droplet,

$$f_n = 4\pi r^2 \frac{dn_{\text{in}}}{dt dA} \quad (6)$$

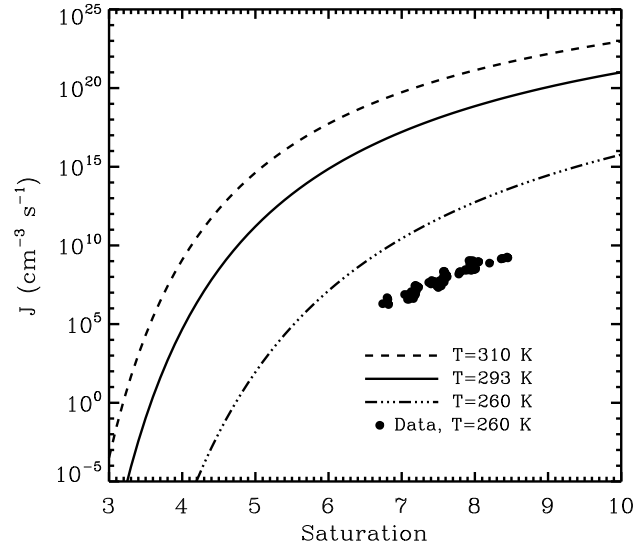


Figure 2. Nucleation rate for water as a function of saturation for three different temperatures: $T = 260 \text{ K}$ (dot-dashed line); $T = 293 \text{ K}$ (solid line), and $T = 310 \text{ K}$ (dashed line). Experimental results from Wölk & Stray (2001) for $T = 260 \text{ K}$ are shown with solid dots.

is the attachment rate for the droplet with $n = (4\pi/3) r^3/v_0$ molecules, and

$$g_n = 4\pi r^2 \frac{dn_{\text{out}}}{dt dA} \quad (7)$$

is the detachment rate for the same droplet. Equation 5 is quite complex. We refer to K00 for a more detailed discussion. We here simply notice that since the detachment and attachment rates enter only through their ratio, the stationary distribution does not depend on the unknown sticking coefficient k_s .

Another fundamental result of the kinetic approach is the nucleation rate J , i.e., the rate at which new nuclei of the condensed phase are created in the vapor. It reads (K00):

$$J = n_X f_1 \left[1 + \sum_{i=2}^{\infty} \left(\prod_{j=2}^i \frac{g_j}{f_j} \right) \right]^{-1} \quad (8)$$

and it now depends linearly on the sticking coefficient k_s through f_1 . In Eq. 5 and 8, the infinite limits of summation can be substituted to summation up to twice the number of molecules in the critical cluster (as long as only the distribution up to the critical cluster is of interest). Finally, Eq. 5 and 8 are valid in the nucleation stage, i.e., when the grain growth and destruction proceeds through attachment or detachment of monomers. In the coalescence stage, when grain-grain collisions are relevant, different equations must be adopted.

Figure 2 shows the nucleation rate as a function of saturation S for water droplets in vapor. The radius of the critical cluster is computed inverting equating the attachment and detachment rates (Eq. 1 and 4) and reads:

$$r_{\text{cr}} = \frac{2\sigma v_0}{kT \ln S} \quad (9)$$

The fact that the nucleation rate increases with saturation is a direct consequence of the decrease of the critical radius.

² <http://www.cheric.org/research/kdb/hcprop/cmprch.php>

A smaller critical radius requires less statistically unfavored random associations to reach the stable configuration and therefore increases the nucleation rate. In Eq. 8, the values of f_i are directly proportional to saturation, while the g_i do not depend on S . This difference brings about, at the mathematical level, the dependence of the nucleation rate on saturation. Three temperatures are shown in Fig. 2: $T = 293$ K (solid), $T = 260$ K (dash-dot) and $T = 310$ K (dashed). The solid dots show the result of a water nucleation experiment (Wölk & Stray 2001) at $T = 260$ K. The comparison of the theory with the data shows that there is a discrepancy of several orders of magnitude between data and experiment. This could be due to $k_s \ll 1$. However, such an explanation is unlikely for water droplets (see Batista et al. 2005). It is rather believed that the discrepancy is due to the failure of the capillary approximation for droplets with a very small n . A larger surface tension for small droplets is required to make the theory consistent with observations. When commenting the quantitative results of the nucleation theory, we shall keep in mind that reality may differ by few orders of magnitude from the theory.

3 THERMAL BALANCE

All the theoretical framework discussed in the above section was developed in an attempt to describe natural and laboratory evidence of nucleation (e.g. rain). In the astrophysical environment, conditions can be very different from the laboratory and the theory needs some adjustments. First we consider that, in general, astrophysical vapors are immersed in an overwhelming quantity of inert H atoms (or, at least, inert in the condensation process). Second, at astrophysical densities the dust particles are at a lower temperature than the gas phase. In this section, we compute the effect of the non thermal equilibrium between gas and droplets (hereinafter dust grains). There are several components affecting the grain temperature, the most important ones are heating by collisions with gas phase particles and heating/cooling through the interaction with the radiation field.

We here consider two effects: heating by collisions with gas particles and cooling due to the emission of radiation. We neglect radiation heating, i.e. we assume the radiation field is diluted and unimportant (radiation is a sink of energy). The cooling due to radiation is given by:

$$\frac{dE}{dt} = 4\pi r^2 \sigma_{\text{SB}} \mathcal{A}(r, T_s) T_s^4 \quad (10)$$

where $\sigma_{\text{SB}} = 5.67 \times 10^{-5}$ erg cm $^{-2}$ K $^{-4}$ s $^{-1}$ is the Stefan-Boltzmann constant, $\mathcal{A} \leq 1$ a factor that takes into account that the grain does not emit as a black body at all frequencies and T_s is the temperature of the grain. $\mathcal{A}(r, T)$ is given by (Laor & Draine 1993):

$$\mathcal{A}(r, T) = \frac{\int Q_{\text{abs}}(\lambda) B_\lambda(T) d\lambda}{\int B_\lambda(T) d\lambda} \quad (11)$$

where $Q_{\text{abs}}(\lambda)$ is the absorption efficiency and $B_\lambda(T)$ is the black-body spectrum.

To compute the heating of the grain due to collisions, we consider the astrophysical scenario, where most of the collision between the grain and the gas particles do not lead to attachment because of the overwhelming abundance of H

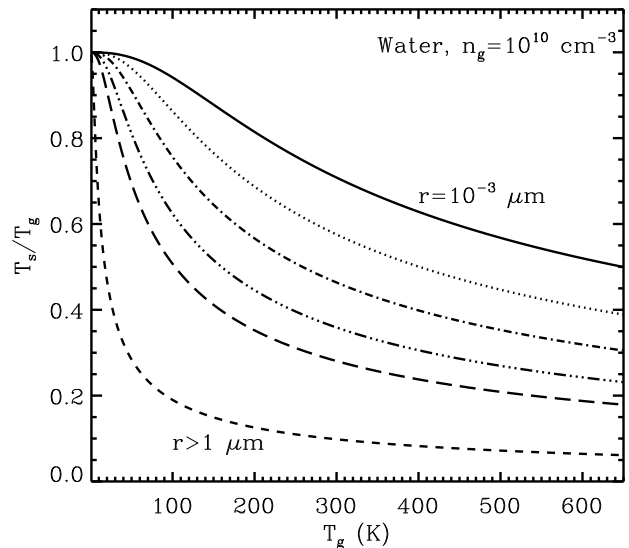


Figure 3. Temperature of water droplets in a vapor as a function of the vapor temperature T_g . The temperature depends on the droplet radius since the radiation emitted is proportional to the droplet opacity, which scales linearly with the radius. From top to bottom, the lines show droplets of radius: 10^{-3} , 3×10^{-3} , 10^{-2} , 3×10^{-2} , 10^{-1} and $\geq 1 \mu\text{m}$. These radii correspond to 3, 10, 30, 100, 300, and 3000 inter-molecular distances, respectively.

over the grain monomers. We also neglect vibrational and rotational energy of the gas particles (again, we suppose to be dominated by H). Finally, we neglect the sputtering of monomers from the cluster that can result from the collision with a high speed gas particle. Such effect is known to be relevant in shock destruction of dust particles but is usually neglected in the classical theory of nucleation (K00). A detailed treatment of the effect requires a detailed description of the energy levels of the clusters, a formidable task that is beyond the scope of this paper. We obtain:

$$\frac{dE}{dt} = 4\pi r^2 \int_0^\infty \frac{n_g v}{4} p(v) \left(\frac{1}{2} \mu m_H v^2 - \frac{3}{2} k T_s \right) dv \quad (12)$$

$$= 4\pi r^2 \sqrt{\frac{2kT_g}{\pi \mu m_H}} n_g k T_g \left(\frac{T_g - T_s}{T_g} \right) \quad (13)$$

where $p(v)$ is the Maxwellian distribution of velocities, m_H is the hydrogen mass, and $\mu \sim 1.2$ the mean atomic weight of the gas. The subscript s always refer to the solid (grain) phase, while the suffix g always refers to the gas (vapor) phase.

The balance between losses and gains of energy gives us an implicit equation for the temperature of the grain as a function of the gas pressure and temperature. Assuming a single equilibrium temperature for small grains is an oversimplification (Guhathakurta & Draine 1989). A broad range of temperatures would likely increase the nucleation rate since the colder-than-average grains could grow into stable grains even for conditions where the average temperature would not allow for nucleation. On the other hand, hotter-than-average grains would be destroyed, providing a balancing effect. Neglecting the temperature distribution we obtain:

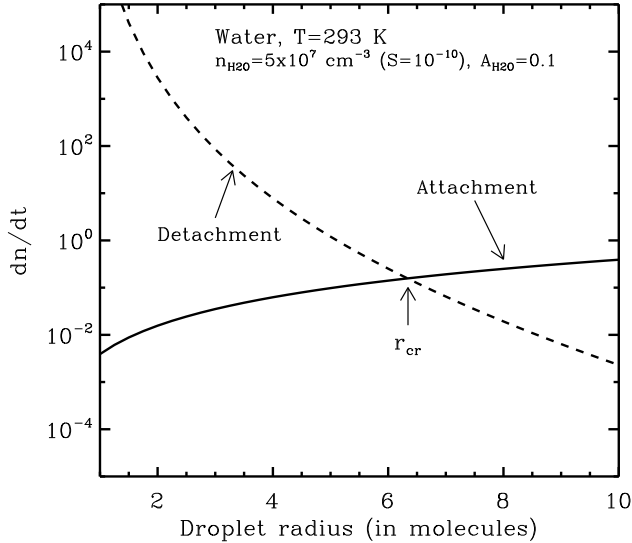


Figure 4. Same as Fig. 1 but for an sub-saturated vapor. Nucleation is still possible due to the cooling of the droplet. A critical radius can be found in this case, analogously to the classical nucleation scenario.

$$\mathcal{A}(r, T_s) T_s^4 = \left(\frac{2kT_g}{\pi\mu m_H} \right)^{1/2} \frac{n_g k T_g T_g - T_s}{\sigma_{SB} T_g} \quad (14)$$

Figure 3 shows the magnitude of the effect for water droplet in a hydrogen dominated gas of total density $n_g = 10^{10} \text{ cm}^{-3}$. For the largest size we used the approximation $\mathcal{A} = 1$, while for small water droplets we adopted the approximation:

$$\mathcal{A}(r, T) \simeq 1 - e^{-r\tau_r} \simeq r\tau_r; \quad r \ll \tau_r^{-1} \quad (15)$$

where τ_r is the opacity per unit length in the medium. For pure water we have $\mathcal{A}(r) \simeq 1200 r$ in the temperature range $250 < T < 600 \text{ K}$ (pure water absorption coefficients are taken from the Oregon Medical Laser Center-OMLC web page³).

4 KINETIC EQUILIBRIUM

As noted by Draine (1981), the departure from thermal equilibrium can have important effects on the kinetic balance of the clusters. Even though the effect of the grain radiative cooling is not exceedingly large (see Fig. 3), especially for the small grains, the detachment rates change exponentially with temperature. This implies that even a small temperature change can make the difference between a nucleating mixture and a non-nucleating one. An additional complication is caused by the fact that while the grain temperature depends on the total gas density n_g , the attachment rate depends on the partial gas density of the compound of interest $n_X = \Xi_X n_g$, where we have defined the number abundance of the compound Ξ_X .

Figure 4 shows the effect of the temperature change in the dynamic equilibrium for water droplets in a vapor with temperature $T_g = 293 \text{ K}$, $n_g = 5 \times 10^8 \text{ cm}^{-3}$, and

$\Xi_{H_2O} = 0.1$. In such conditions, the saturation⁴ is $S = 10^{-10}$ and the vapor should not nucleate. Indeed, for $T_s = T_g$, the detachment rate would be $\sim 10^{10}$, about ten orders of magnitude larger than the attachment rate, and droplets would evaporate. Due to the approximately exponential dependence of the experimental saturation density with temperature, the change in temperature of the droplets suppresses the detachment rate. The situation appears now qualitatively similar to the nucleating condition in Fig. 1. At small radii, the detachment rate is larger than the attachment rate, and the droplets evaporate. A critical radius r_{cr} does exist, where the two rates are identical and the droplet is in equilibrium. The critical radius is now given by a modified version of Eq. 9, since the gas and grain temperatures are different:

$$r_{cr} = \frac{2\sigma v_0}{kT_s \ln Z} \quad (16)$$

where

$$Z = \frac{n_X}{n_{X,eq}(T_s)} \sqrt{\frac{T_g}{T_s}} \quad (17)$$

In the same way as in the LTE case, droplets larger than the critical radius grow due to the larger attachment rate with respect to the detachment rate.

Figure 4 was computed solving numerically Eq. 14 for the temperature with $\mathcal{A}(r, T)$ obtained from Eq. 11 with water data taken from the OMLC web page (see footnote 3). Again, $k_s = 1$ was assumed. Relaxing this assumption would change the normalization of the two curves so that r_{cr} would remain constant.

5 NUCLEATION

The nucleation rate for the sub-saturated nucleating vapor can be computed using Eq. 8 given the attachment rate for the gas temperature and the detachment rate computed at the grain temperature. Figure 5 shows an extension of Fig. 2 to much lower saturations (and therefore densities). When saturation drops below unity, nucleation does not take place, until at very low densities and saturations non-LTE nucleation sets in. The nucleation rate is somewhat small, since the attachment rate is low at low saturation, but the detachment rate is suppressed by the decreased temperature of the grains and therefore nucleation is possible. It must be emphasized that the theory becomes more and more inaccurate as we approach the limit of a small number of monomers in the critical cluster. In this case, many of the approximations made to derive the theory lose validity. First, the opacity per unit length loses meaning, and the cooling rate is not computed accurately. Second, the cluster does not have a well-defined surface any more and the capillary approximation for the surface tension breaks down. For this reason we did not include in Fig. 5 the very low saturation limit, since the number of monomers in the critical cluster becomes close to unity. Nucleation is still possible there, but computing the rate in the atomistic approximation is beyond the goal of

⁴ The saturation is defined as $S = n_X/n_{X,eq}(T_g)$ also in non-LTE conditions, but $S = 1$ loses in this case the meaning of threshold for the nucleation process.

³ <http://omlc.ogi.edu/spectra/water/>

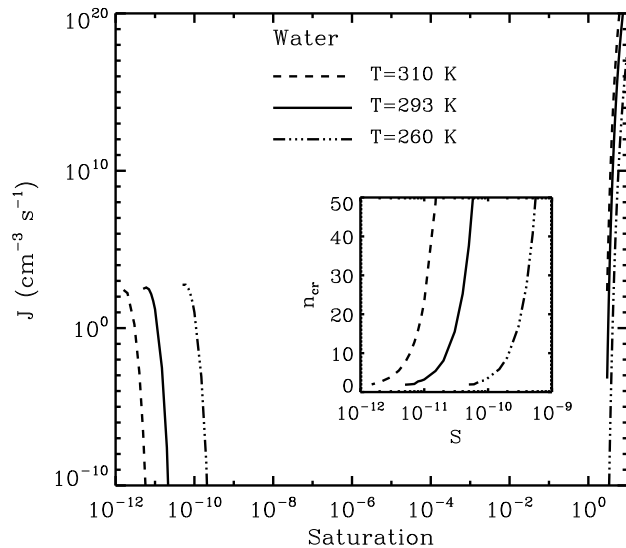


Figure 5. Same as Fig. 2 but extended to very low saturation. The nucleation rate is non-negligible and nucleation is possible. The inset shows the number of monomers in the critical cluster as a function of saturation. Contrary to the classical case, the critical radius increase with the saturation, in this case. The curves on the right side of the plot are the results for LTE nucleation from Fig. 2.

this paper and, for what matters, a very controversial issue. We show in the inset of Fig. 5 the number of monomers in the critical cluster as a function of saturation in the non-LTE nucleating region. Calculation have been stopped at the limit $n_{cr} = 2$, but for $n_{cr} \lesssim 5$ the results should be taken with caution.

Finally, we show in Fig. 6 the new conditions for water droplet nucleation in the $n - T$ plane. As explained above, nucleation in the non-LTE area depends on the abundances Ξ_{H_2O} . In dark gray we show the region where nucleation is possible in the classical view. In light gray, we show the area where non-LTE nucleation is possible in the limit $\Xi_{H_2O} \rightarrow 1$. Solid lines show how the area is modified in the cases of $\Xi_{H_2O} = 10^{-1}$, 10^{-3} , and 10^{-5} . The three thin vertical lines in the lower left part of the diagram show the conditions under which nucleation rates have been computed in Fig. 5. It is important to note that even though nucleation is possible at higher densities, the nucleation rate becomes non-negligible only for densities roughly equal or smaller than $n_{H_2O} = 10^8 \text{ cm}^{-3}$. The dependence of nucleation on density, for a given temperature, is quite complex. At very high densities, the conditions of temperature equilibrium are maintained by the high rate of collisional heating and classical LTE nucleation takes place. As the density is decreased, two different things can happen. At high temperature (the region in Fig. 6 and 7 where a white area is present), the vapor becomes sub-saturated and nucleation is halted. Decreasing the density even further allows for the cooling of the sub-critical grains, and nucleation in non-LTE sets in. If the temperature is lower, non-LTE conditions apply even in saturated vapors. In that case, the vapor is always nucleating (see Fig. 8). The dashed line in Fig. 6 shows the region where the temperature of the droplets is equal to the freezing point of water (assuming it freezes at 0°C independent

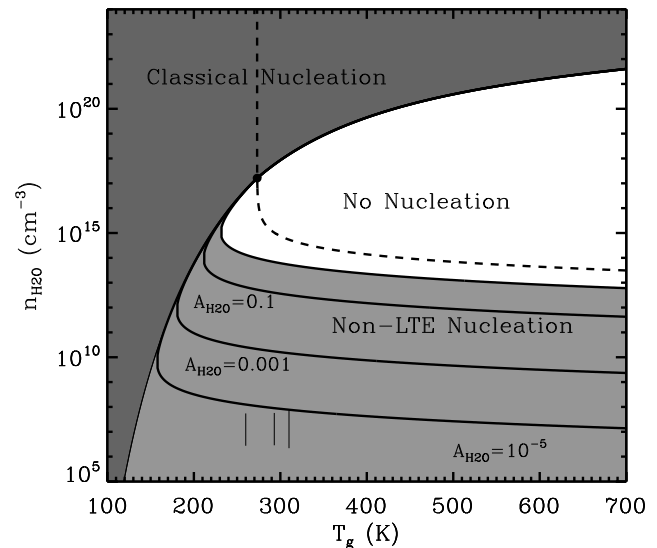


Figure 6. Nucleation phase diagram for water droplets. The classical vapor pressure line is shown as a thin solid line. The new equilibrium is shown as a thick solid line. Only the region inside the line does not produce any nucleation. The three thin vertical lines in the lower left corner show the values for which the nucleation rate is shown in Fig. 5. The dashed line shows the ice formation boundary: only the droplets in the upper right corner are liquid (assuming that water freezes at 273.15 K independently of pressure).

dent on pressure). Non-LTE nucleation results therefore in ice and not liquid droplets. Finally, the above treatment is valid only if there are no pre-existing grains (e.g. graphite or silicates) that can work as seeds for heterogeneous nucleation. In that case, the presence of already cold grains could result in the growth of ice mantels rather than in the nucleation of new droplets.

5.1 Graphite

Even though water has an astrophysical relevance for dust, especially in covering refractory grains with ice mantles, we now consider a more pregnant example: graphite grains condensing from carbon atoms in the gas phase. For simplicity, we consider a gas made only of hydrogen with solar carbon abundance: $\Xi_C = 3.3 \times 10^{-4}$ (Grevesse & Sauval 1998). We use the vapor pressure measurement from Brewer, Gilles & Jenkins (1948) and the surface tension $\sigma_C = 34.6 \text{ dyne/cm}$ (Morcos 1972).

Figure 7 is analogous to Fig. 6, but shows the phase diagram of graphite. Note also that the y-axis reports the total density of the gas and not the partial density of carbon atoms. Analogously to the case of water, we see that graphite grains can form in non-LTE at temperatures much larger than in the classical scenario.

To compute nucleation rates in non-LTE, we need to derive the factor \mathcal{A} for graphite. We use the tables⁵ of Q_{abs} from Draine & Lee (1984) and Laor & Draine (1993). In some cases, however, the grain sizes given in the tables are

⁵ <http://www.astro.princeton.edu/~draine/dust/dust.diel.html>

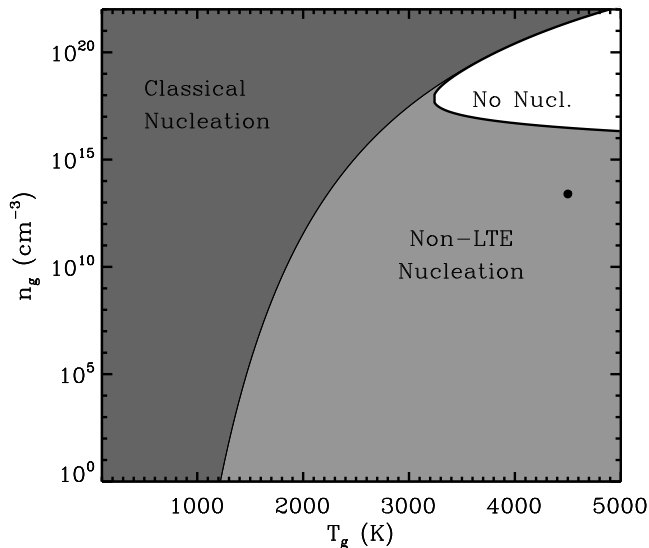


Figure 7. Nucleation phase diagram for graphite grain in a hydrogen gas with carbon number abundance $\Xi_C = 3.3 \times 10^{-4}$. As for the case of water analyzed above, there exist a big region at high temperatures and low densities where graphite grains can nucleate in non-LTE conditions with the gas. The point marks the conditions for which the nucleation rate $J \approx 7 \times 10^4 \text{ cm}^{-3} \text{ s}^{-1}$ has been computed in the text.

not small enough (the smallest grain considered in the tables has $r = 0.001 \mu\text{m}$ while the smallest we consider has $r = 0.00013 \mu\text{m}$). In that case we extrapolate to smaller radii in the optically thin limit assuming $Q_{\text{abs}}(\lambda, r) = 1 - \exp(-r\tau_r)$.

In the case of graphite, nucleation in the non-LTE region can be very efficient. For a gas density $n_g = 2.5 \times 10^{13} \text{ cm}^{-3}$ and temperature $T_g = 4500 \text{ K}$ (see solid dot in Fig. 7), the critical cluster has ≈ 7 carbon atoms and the nucleation rate is $J \approx 7 \times 10^4 \text{ cm}^{-3} \text{ s}^{-1}$.

Another important aspect of Fig. 7 is that there is a vast temperature range where there is no non-nucleating region between the classical and non-LTE nucleating regions. This was true for water as well, but in a narrower region. For $T_g < 3250 \text{ K}$ in the carbon-hydrogen mixture considered, the grain temperature is smaller than the gas temperature even in the classical nucleating region. This implies that the nucleation rate is different from the classical value and the cooling of the grains has to be considered even in the classical region. Figure 8 shows the nucleation rate for $T = 2500 \text{ K}$ in the saturation range $0.1 \leq S \leq 10$. Even though a mixture in true equilibrium does nucleate for $S > 1$, non-LTE effects increase the rate.

6 DISCUSSION AND CONCLUSIONS

We have considered the effect of grain (cluster, droplet) cooling in the nucleation of liquid and solid phases in vapors. We find that the effect can be dramatic on the nucleation rate and on the nucleation phase diagram, allowing for nucleation in large regions of the parameter space that are classically considered to be non-nucleating.

As is in general true for nucleation, there are several limits and approximations that we should bear in mind when

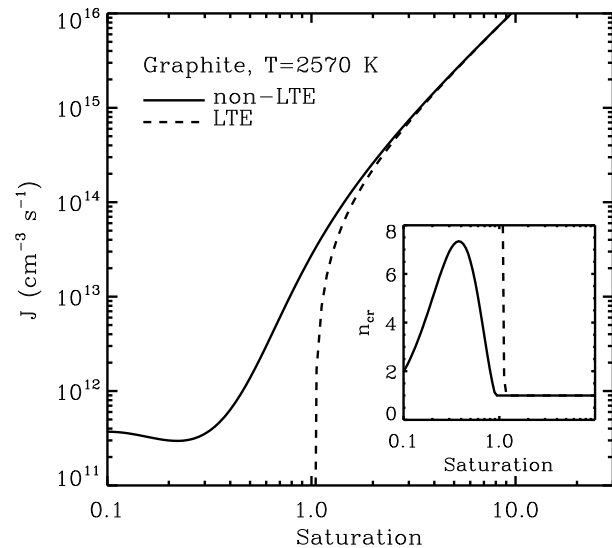


Figure 8. Nucleation rate in a carbon-hydrogen mixture with solar carbon abundance at $T = 2570 \text{ K}$. The dashed line shows the classical result for “true equilibrium” nucleation, while the solid line shows the result of non-LTE nucleation. Even for $S \gtrsim 1$, where LTE nucleation takes place, allowing for the grain cooling increases the nucleation rate. The inset shows the number of monomers in the critical cluster for the two cases as a function for the saturation. Note that computations in the super-saturated regime suffer the uncertainties of the few monomers limit for both LTE and non-LTE assumptions.

considering the theory from the quantitative point of view. As exemplified by the comparison of the data with the theory in Fig. 2, several orders of magnitude can separate the nucleation rate prediction from the observations. The controversial points are:

- *Sticking coefficients* — Most of the figures and computations in this work assume $k_s = 1$. This is not always true (Batista et al. 2005). In addition to its dependence on temperature, the sticking coefficient may depend on the size of the cluster. A big cluster could more easily absorb the extra kinetic energy of the incoming monomer, compared to a small cluster (K00), and therefore k_s may be significantly smaller than unity for very small clusters.

- *Capillary approximation* — The capillary approximation, i.e., the assumption that the surface tension does not depend on the cluster size, is very controversial, and a change in the surface energy for very small clusters could result in big changes on the nucleation rate. For example, the discrepancy in Fig. 2 could be solved by assuming a larger surface tension for the very small water droplet. In addition, macromolecules do not even have a properly defined surface, and the whole concept does not apply. Finally, the exponential factor in Eq. 3 depends on the assumption that the clusters are spherical. A different ratio of the surface to the volume would modify this term. This is likely for small graphite clusters, since graphite tends to aggregate in a planar form.

- *Detachment rate for small clusters* — In this paper, and in most nucleation theory, the detachment rate is computed by propagating to very small clusters the detachment rate of macroscopic bodies. It is very likely that, in the very small

limit, the detachment is governed by completely different processes. Let us analyze the two limits. For a macroscopic body, the number of monomers is so large that monomers with a statistically higher energy can detach since their energy is larger than the binding energy. In the opposite limit of a dimer, the detachment has to be due to an external action: either a collision with a fast monomer or with a photon or with another cluster. In this limit destructive collisions have to be considered.

- *Cooling of macromolecules* — This is a new problem that arises when the cooling of the grains is considered. We have assumed that the grains cool as modified black bodies down to the smallest sizes. When the number of monomers in the cluster becomes small, the cooling will not be through a continuum spectrum, but through lines and bands. A more refined treatment of cooling is necessary to compute accurate nucleation rates.

- It should finally be kept in mind that we allowed for the complete cooling of the grains, neglecting the effects of a background radiation field in setting a lower limit to the temperature. In addition, we neglected the fact that the temperature of small grains is largely stochastic and that at high temperature some collisions between grains and gas particles can result in sputtering rather than accretion.

Despite all these caveats, the main result of this paper holds: the region where a vapor spontaneously nucleate is not limited to the classic region, when nucleation takes place in thermal equilibrium and $T_g = T_s$. Allowing for the clusters to cool inhibits the detachment of monomers from the clusters and allow for nucleation at higher temperatures and lower densities than in the classical scenario. The nucleation rates tend to be orders of magnitude smaller than those derived in thermal equilibrium, but provide a non-negligible correction to the LTE rate for mildly super-saturated vapors with $S \gtrsim 1$, especially at low temperature.

In the astrophysical scenario small nucleation rates are not a big worry. The ISM of our Galaxy contains approximately 1 per cent of its mass in dust grains (Mathis et al. 1977). This corresponds to approximately one dust particle every cubic meter (assuming a power-law grain size distribution as in Mathis et al. 1977). However, in the present day Universe the ISM is already polluted with dust and in the presence of seed grains it is likely that the process of mantle growth dominates over non-LTE nucleation in the diffuse medium. The process of non-LTE nucleation may therefore be important at high redshift, when the ISM is first polluted with metals by supernova explosions. It is unclear if supernovæ do generate dust by themselves, and even more whether the generated dust can survive the sputtering in the forward-reverse shock systems (Bianchi & Schneider 2007; Nath, Laskar & Shull 2007). In the case that supernovæ do mainly pollute the ISM with metals but with no or a negligible quantity of dust, non-LTE nucleation could become the dominant process of dust nucleation in the early universe. Detailed estimates of nucleation in the various scenarios require a more detailed understanding of the properties of the very small nuclei and are beyond the scope of this paper.

ACKNOWLEDGEMENTS

I thank the anonymous referee for a thorough review and constructive comments that improved the contents of this paper. I am grateful to Mike Shull, Nahum Arav and Bruce Draine for useful suggestions and discussions.

REFERENCES

- Abraham F. F., 1974, Homogeneous nucleation theory, Academic Press, New York
- Batista E. R., Ayotte P., Bilić A., Kay B. D., Jónsson H., 2005, PRL, 95, 223201
- Becker R., Döring W., 1935, Ann. Physik, 24, 719
- Bianchi S., Schneider R., 2007, MNRAS, 378, 973
- Brewer L., Gilles P. W., Jenkins F. A., 1948, J. Chem. Phys., 16, 797
- Cardelli J. A., Clayton G. C., Mathis J. S., 1989, ApJ, 345, 245
- Draine B. T., 1979, Ap&SS, 65, 313
- Draine B. T., 1981, ASSL, 88, 317
- Draine B. T., Lee H. M., 1984, ApJ, 285, 89
- Draine B. T., 1989, eidr.proc, 103
- Draine B. T., 2003, ARA&A, 41, 241
- Edmunds M. G., 2001, MNRAS, 328, 223
- Elvis M., Marengo M., Karovska M., 2002, ApJ, 567, L107
- Feder J, Russell K. C., Lothe J., Pound G. M., 1966, Advances in Physics, 15:57, 111
- Gail H.-P., Sedlmayr E., 1986, A&A, 166, 225
- Grevesse N., Sauval A. J., 1998, Space Science Reviews, 85, 161
- Kashkiv D., 2000, “Nucleation: basic theory with applications”, Butterworth-Heinemann, Oxford
- Kozasa T., Hasegawa H., Nomoto K., 1989, ApJ, 344, 325
- Kozasa T., Hasegawa H., Nomoto K., 1991, A&A, 249, 474
- Laor A., Draine B. T., 1993, ApJ, 402, 441
- Mathis J. S., Rumpl W., Nordsieck K. H., 1977, ApJ, 217, 425
- Mathis J. S., 1990, ARA&A, 28, 37
- McKee C., 1989, IAUS, 135, 431
- Morcos I., 1972, J. Chem. Phys., 57, 1801
- Nath B. B., Laskar T., Shull J. M., 2007, ApJ submitted
- Nowakowski B., Ruckenstein E., 1991a, J. Chem. Phys., 94, 1397
- Nowakowski B., Ruckenstein E., 1991b, J. Chem. Phys., 94, 8487
- Nozawa T., Kozasa T., Umeda H., Maeda K., Nomoto K., 2003, ApJ, 598, 785
- Salpeter E. E., 1977, ARA&A, 15, 267
- Schneider R., Ferrara A., Salvaterra R., 2004, MNRAS, 351, 1379
- Stein W. A., Soifer B. T., 1983, ARA&A, 21, 177
- Todini P., Ferrara A., 2001, MNRAS, 325, 726
- Vehkamäki H. 2006, “Classical nucleation theory in multicomponent systems”, Springer, Heidelberg
- Weingartner J. C., Draine B. T., 2001, ApJ, 548, 296
- Wölk J., Strey R., 2001, J. Phys. Chem. B, 105, 11683